Molecular Basis of Cell and Developmental Biology:

Conditional Deletion of Gremlin Causes a Transient Increase in Bone Formation and Bone Mass

Elisabetta Gazzerro, Anna Smerdel-Ramoya, Stefano Zanotti, Lisa Stadmeyer, Deena Durant, Aris N. Economides and Ernesto Canalis

J. Biol. Chem. 2007, 282:31549-31557.
doi: 10.1074/jbc.M701317200 originally published online September 4, 2007

THE JOURNAL OF BIOLOGICAL CHEMISTRY VOL. 282, NO. 43, pp. 31549–31557, October 26, 2007

Conditional Deletion of Gremlin Causes a Transient Increase in Bone Formation and Bone Mass*

Received for publication, February 15, 2007, and in revised form, August 2, 2007 Published, JBC Papers in Press, September 4, 2007, DOI 10.1074/jbc.M701317200

Elisabetta Gazzerro[‡§1], Anna Smerdel-Ramoya[‡§1], Stefano Zanotti[‡], Lisa Stadmeyer[‡], Deena Durant[‡], Aris N. Economides[¶], and Ernesto Canalis[‡§2]

From the [‡]Department of Research, Saint Francis Hospital and Medical Center, Hartford, Connecticut 06105-1299, the [§]University of Connecticut School of Medicine, Farmington, Connecticut 06030, and [¶]Regeneron Pharmaceuticals, Inc., Tarrytown, New York 10591

Gremlin is a glycoprotein that binds bone morphogenetic proteins (BMPs) 2, 4, and 7, antagonizing their actions. Gremlin opposes BMP effects on osteoblastic differentiation and function *in vitro* and *in vivo*, and its overexpression causes osteopenia. To define the function of gremlin in the skeleton, we generated *gremlin 1* (*grem1*) conditional null mice by mating mice where *grem1* was flanked by *lox*^{P} sequences with mice expressing the Cre recombinase under the control of the osteocalcin promoter. *grem1* null male mice displayed increased trabecular bone volume due to enhanced osteoblastic activity, because mineral apposition and bone formation rates were increased. Osteoblast number and bone resorption were not altered. Marrow stromal cells from *grem1* conditional null mice expressed higher levels of alkaline phosphatase activity. Gremlin down-regulation by RNA interference in ST-2 stromal and MC3T3 osteoblastic cells increased the BMP-2 stimulatory effect on alkaline phosphatase activity, on Smad 1/5/8 phosphorylation, and on the transactivation of the BMP/Smad reporter construct 12×SBE-Oc-pGL3. Gremlin down-regulation also enhanced osteocalcin and Runx-2 expression, Wnt 3a signaling, and activity in ST-2 cells. In conclusion, deletion of *grem1* in the bone microenvironment results in sensitization of BMP signaling and activity and enhanced bone formation *in vivo*.

Bone morphogenetic proteins (BMPs)[3] are important determinants of cell fate and play a central role in the regulation of osteoblastogenesis and endochondral bone formation (1). BMPs, in conjunction with Wnt, induce the differentiation of mesenchymal cells toward the osteoblastic lineage and enhance the pool and function of mature osteoblasts (2–4). Upon ligand binding, BMPs initiate a signal transduction cascade activating the mothers against the decapentaplegic (Smad) or mitogen-activated protein kinase signaling pathways (1, 5–8). In osteoblastic cells, Wnt binding to specific receptors and co-receptors leads to the stabilization of β-catenin and its translocation to the nucleus, where it associates with nuclear factors to regulate transcription (4, 9, 10).

The effects of BMPs and Wnt are controlled by a large group of secreted polypeptides that prevent BMP or Wnt signaling by binding BMPs or Wnt, or their receptors/co-receptors, precluding ligand-receptor interactions (1, 4, 11, 12). The binding affinity and selectivity of secreted antagonists for specific BMPs varies, and selected antagonists can have dual BMP and Wnt antagonistic activity (1, 13–16).

Gremlin and its rat homolog, down-regulated by v-*mos* (*drm*), are secreted glycoproteins with a molecular mass of 20.7 kDa (17–19). *Gremlin 1* (*grem1*) is a member of the differentially screening-selected gene aberrative in neuroblastoma (*dan*)/*cerberus* family of genes, and gremlin was originally identified as a dorsalizing agent, with BMP antagonistic activity, in *Xenopus* embryos (1, 17). Gremlin binds and prevents the activity of BMP-2, -4, and -7. Gremlin is expressed by stromal cells surrounding certain neoplastic cells, and it is considered to play a role in cell survival and possibly tumorigenesis (19, 20). Homozygous null mutations of the *grem1* gene in mice result in serious developmental limb, metanephric, and lung abnormalities, leading to absent kidneys and intrauterine or newborn lethality (21, 22). The patterning of distal limb skeletal elements is tightly regulated by the reciprocal interactions between BMPs, fibroblast growth factors (FGFs) 4 and 8, and Sonic hedgehog (SHH) (21). By inhibiting BMP action, gremlin allows for FGF 4/8 expression, which in turn promotes SHH expression in the posterior limb bud, which is required for proper limb patterning and development.

Later in skeletal development, after the pattern of skeletal elements has been established, *grem1* is expressed by osteoblasts (23). Transgenic mice overexpressing gremlin under the control of the osteocalcin promoter exhibit severe osteopenia secondary to decreased bone formation (24), consistent with the role of gremlin as a BMP antagonist. Gremlin binds and inhibits BMP signaling and activity in cells of the osteoblastic lineage, and tempers Wnt signaling (24). This is in accordance

* This work was supported by Grant AR21707 from NIAMS, National Institutes of Health (to E. C.), and a fellowship award from the Arthritis Foundation (to E. G.). The costs of publication of this article were defrayed in part by the payment of page charges. This article must therefore be hereby marked "*advertisement*" in accordance with 18 U.S.C. Section 1734 solely to indicate this fact.

[1] Both authors contributed equally to this work.

[2] To whom correspondence should be addressed: Dept. of Research, Saint Francis Hospital and Medical Center, 114 Woodland St., Hartford, CT 06105-1299. Tel.: 860-714-4068; Fax: 860-714-8053; E-mail: ecanalis@stfranciscare.org.

[3] The abbreviations used are: BMP, bone morphogenetic protein; APA, alkaline phosphatase activity; BAC, bacterial artificial chromosome; BMD, bone mineral density; CMV, cytomegalovirus; *Dan*, differentially screening-selected gene aberrative in neuroblastoma; *drm*, down-regulated by v-*mos*; ES, embryonic stem; ERK, extracellular regulated kinases; FGF, fibroblast growth factor; FRT, flippase recombinase target; GAPDH, glyceraldehyde-3-phosphate dehydrogenase; Lef-1/Tcf-4, lymphoid enhancer binding factor/T cell-specific factor; MAP, mitogen activated protein; Smad, mothers against decapentaplegic; Neo, neomycin phosphotransferase; RT, reverse transcription; RNAi, RNA interference; Runx-2, runt-related transcription factor 2; SHH, sonic hedgehog; siRNA, small interfering RNA.

with the dual, BMP and Wnt, inhibitory activity reported for other members of the *dan/cerberus* family of genes (1, 15, 16).

Null mutations of *grem1* nearly always cause embryonic lethality, not allowing for the study of their adult skeletal phenotype (21, 22). In the present study, a conditional *grem1* deletion to inactivate gremlin in the bone environment post-natally was used. For this purpose, genetically engineered mice, where the coding sequence of *grem1* was flanked by lox^P sequences, were created and crossed with transgenic mice expressing the Cre recombinase under the control of the human osteocalcin promoter, and their skeletal phenotype was determined. In addition, mechanisms of gremlin action were explored *in vitro*, following its down-regulation in ST-2 stromal and MC3T3 osteoblastic cells using RNA interference (RNAi).

EXPERIMENTAL PROCEDURES

Conditional Deletion of grem1—To generate a conditional-null allele of *grem1*, a segment of exon 2, where the coding sequence of *grem1* resides in its totality, was flanked with lox^P sequences to allow the excision of the entire open reading frame by Cre recombination (Fig. 1, *A* and *B*). Targeted embryonic stem (ES) cells harboring a lox^P-flanked allele for $grem1^{loxP/+}$ were generated using Velocigene™ technology (25). Briefly, a bacterial artificial chromosome (BAC) containing mouse genomic DNA encompassing *grem1* sequences was selected by PCR screen from a 129/SvJ mouse BAC library containing ~140 kb of genomic DNA (Release I, BAC id 427a3, Incyte Genomics, Wilmington, DE). To generate the targeting vector, BAC 427a3 was modified using bacterial homologous recombination in a three-step process as follows: 1) a lox^P site was introduced in a non-conserved region 335 bp upstream of exon 2, by inserting a LoxP_I-SceI_EM7-Zeo_I-SceI cassette; 2) the I-SceI_EM7-Zeo_I-SceI cassette was removed from the modified BAC by restricting with I-SceI, re-ligating, and selecting for modified BACs that had lost the Zeo cassette while retaining the LoxP_I-SceI sequence upstream of exon 2; and 3) a lox^P site was inserted 550 bp downstream of the stop codon of *grem1* as part of a flippase recombinase target (FRT)-flanked-phosphoglycerate kinase (PGK)-neomycin phosphotransferase (Neo)-polyA_FRT_LoxP cassette, while simultaneously deleting 66 bp (GATGGCAAACGGGACAGAGGACTGACGCAGGAACGGTCAGGCTGAGGACCAGTCGGCCAGTGA) of non-conserved exon 2 sequence, to accommodate PCR probes for genotyping by loss of native allele assay (25, 26). Using restriction mapping, it was determined that the modified BAC had homology arms of ~70 kb adjoining the lox^P-flanked allele, and the modified BAC was used as a vector to target *grem1* in an F1 (129SvJ/C57BL/6) hybrid ES cell line (25, 26). Genotyping of ES cell clones using loss of native allele assay revealed that 12 of 288 clones screened were targeted, indicating a targeting frequency of ~4.2%. Two independent targeted ES cell lines were used to generate male chimeric mice. Chimeras that were complete transmitters of ES-derived sperm were bred to C57BL/6 females to generate F1 heterozygous mice, which were genotyped by loss of native allele assay. Heterozygous mice were intermated to create homozygous $grem1^{loxP/loxP}$ mice in a mixed 129SvJ/C57BL/6 genetic background. To ensure that none of the genetic manipulations caused a skeletal phenotype, $grem1^{loxP/loxP}$ were compared with wild type littermate controls.

Transgenic mice overexpressing the Cre recombinase under the control of a 3.9-kb human osteocalcin promoter (Oc-Cre), created in an FVB genetic background, were obtained from T. Clemens (Birmingham, AL) (27). Cre recombinase activity was confirmed in bone tissue by mating osteocalcin Cre transgenics with *lacZ*-expressing, Gtrosa26tm1Sor test mice, and demonstrating β-galactosidase staining in calvariae following the excision of a lox^P-flanked intervening stop codon (not shown) (28).

$Grem1^{loxP}$ mice were studied in a *grem1* heterozygous null background. For this purpose, osteocalcin Cre mice were mated to *grem1* heterozygous ($grem1^{+/LacZ}$) null C57BL/6 mice, obtained from R. Harland (Berkeley), and then intermated for the creation of homozygous osteocalcin Cre mice in a heterozygous $grem1^{+/LacZ}$ null background ($grem1^{+/LacZ}$:*Oc-Cre/Oc-Cre*) (21, 27). These were mated with homozygous $grem1^{loxP/loxP}$ mice, generating an experimental cohort, where Cre deletes the lox^{loxP}-flanked sequences from the $grem1^{loxP}$ allele, and where a *grem1* null allele is retained ($grem1^{\Delta/LacZ}$), and a control littermate cohort carrying a Cre deleted $grem1^{loxP}$ allele and a wild-type allele ($grem1^{\Delta/+}$). To ensure that the latter were appropriate controls, non-conditional *grem1* heterozygous ($grem1^{+/LacZ}$) null mice were compared with wild-type littermate C57BL/6 mice, obtained from heterozygous/wild-type matings, for their skeletal phenotype. Male mice of identical genetic composition were compared at 4 weeks of age, a time of marked expression of the osteocalcin gene, and at 3 months of age. LacZ/β-galactosidase staining of long bones was carried out in 3-day-old mice. Genotyping of $grem1^{loxP}$ mice was carried out in tail DNA by PCR using the common reverse primer, 5′-AAACAGGAGTGGTCAGCA-3′, and the forward primer, 5′-ACGGGACAGAGGACTGA-3′, for the wild-type allele (328 bp), or the forward primer, 5′-GGTGGGGTGGGATTAGATA-3′, for the targeted lox^P allele (696 bp). Genotyping of $grem1^{+/LacZ}$, $grem1^{\Delta/LacZ}$, and $grem1^{\Delta/+}$ mice was carried out by PCR using forward primer, 5′-AAAGGTTCCCAAGGAGCCATTCC-3′, and reverse primer, 5′-AACAGAAGCGGTTGATGATAGTGCG-3′, for the wild-type allele (300 bp), and forward primer, 5′-GGTCAATCCGCCGTTTGTTCC-3′, and reverse primer, 5′-TAGTCACGCAACTCGCCGCACATC-3′, for the targeted LacZ allele (500 bp). Deletion of lox^P flanked sequences by the Cre recombinase was documented by PCR in DNA extracted from calvariae of 1-month-old mice using the forward primer 5′-GGTTGAAAAGTGGGGTCT-3′ and the reverse primer 5′-AAACAGGAGTGGTCA GCA-3′, to create a 670-bp product. *Grem1* deletion was confirmed by determination of gremlin mRNA levels by real-time reverse transcription (RT)-PCR in calvarial extracts. Animal experiments were approved by the Animal Care and Use Committee of Saint Francis Hospital and Medical Center.

X-ray Analysis and Bone Mineral Density—Radiography was performed on anesthetized or sacrificed mice on a Faxitron x-ray system (model MX 20, Faxitron x-ray Corp., Wheeling, IL). The x-rays were performed at an intensity of 30 kV for 20 s. Bone mineral density (BMD, g/cm^2) was measured on anesthetized mice using the PIXImus small animal DEXA system (GE Medical Systems/LUNAR, Madison, WI) (29). Calibrations

were performed with a phantom of a defined value, and quality assurance measurements were performed prior to each use. The coefficient of variation for total BMD was <1% (n = 9 mice).

Bone Histomorphometric Analysis—Static and dynamic histomorphometry was carried out on femurs from experimental and control littermate mice at 1 month and 3 months of age. Mice were injected with calcein, 20 mg/kg, and demeclocycline, 50 mg/kg, at an interval of 2 or 7 days, for 1- or 3-month-old mice, respectively, and sacrificed by CO_2 inhalation 2 days after the demeclocycline injection. Femurs were dissected, fixed in 70% ethanol, dehydrated, and embedded undecalcified in methyl methacrylate. Longitudinal sections, 5 μm thick, were cut on a Microm microtome (Microm, Richard-Allan Scientific, Kalamazoo, MI) and stained with 0.1% toluidine blue, pH 6.4, or Von Kossa. Static parameters of bone formation and resorption were measured in a defined area between 725 μm and 1270 μm from the growth plate, using an OsteoMeasure morphometry system (Osteometrics, Atlanta, GA). For dynamic histomorphometry, mineralizing surface per bone surface and mineral apposition rate were measured in unstained sections under ultraviolet light, as described (24). The bone formation rate was calculated. The terminology and units used are those recommended by the Histomorphometry Nomenclature Committee of the American Society for Bone and Mineral Research (30).

Expression Analysis of the β-Galactosidase Reporter Gene—Whole mount LacZ/β-galactosidase gene expression was analyzed in 3-day-old femurs and tibiae from *grem1*$^{\Delta/LacZ}$ and *grem1*$^{\Delta/+}$ controls (31). Femurs and tibiae were harvested from 3-day-old mice, and fixed in a 0.4% glutaraldehyde at 4 °C overnight. Tissues were rinsed with phosphate-buffered saline and incubated in LacZ staining solution 4 h at 37 °C, decalcified in Decal-Stat (Decal Co., Tallman, NY) 24 h at 4 °C, and embedded in cryomatrix (Thermofisher, Waltham, MA). 5-μm sections were cut on a cryostat and counterstained with eosin and visualized by microscopy.

Bone Marrow Stromal Cell Cultures—Femurs from *grem1*$^{\Delta/LacZ}$ and *grem1*$^{\Delta/+}$ controls were aseptically removed from 4-week-old mice, after CO_2 asphyxiation, and stromal cells were recovered by centrifugation, as described previously (24). Cells were plated at a density of 5×10^5 cells/cm^2 and cultured in minimum essential medium (α-MEM, Invitrogen) containing 15% fetal bovine serum (Atlanta Biologicals, Norcross, GA) at 37 °C in a humidified 5% CO_2 incubator. When cells reached confluence (6–7 days of culture), the medium was changed to α-MEM supplemented with 10% fetal bovine serum, 50 μg/ml ascorbic acid, and 5 mM β-glycerophosphate (Sigma-Aldrich). Cells were cultured for an additional 10- to 16-day period, and serum was deprived overnight, treated with BMP-2 (Wyeth, Collegeville, PA) for 24 h, and analyzed for alkaline phosphatase activity and gremlin mRNA expression.

Culture of Cell Lines and RNA Interference—ST-2 cells, cloned stromal cells isolated from bone marrow of BC8 mice, and MC3T3-E1, osteoblastic cells derived from mouse calvariae, were plated at a density of 10^4 cells/cm^2, and grown in a humidified 5% CO_2 incubator at 37 °C in α-MEM, supplemented with 10% fetal bovine serum (32, 33). To down-regulate gremlin expression *in vitro*, a 19-mer double-stranded small interfering (si) RNA targeted to bp 884–902 of *grem1* mouse DNA sequence was obtained commercially, and a 19-mer silencing scrambled RNA composed of sequences with no homology to known mouse or rat sequences was used as a control (Ambion, Austin, TX) (34, 35). Gremlin or scrambled siRNA, all at 20 nM, were transfected into sub-confluent ST-2 or MC3T3 cells using siLentFect lipid reagent, in accordance with manufacturer's instructions (Bio-Rad, Hercules, CA) (36). To ensure adequate down-regulation, total RNA was extracted in cells 24–96 h following the transfection of siRNAs, and gremlin mRNA levels were determined by real-time RT-PCR. To test for effects on osteoblastic function, transfected cells were allowed to recover for 24 h, and treated with recombinant human BMP-2 or Wnt 3a (R&D Systems, Minneapolis, MN) for 72 h in the presence of 5 mM β-glycerophosphate and ascorbic acid (Sigma-Aldrich) and analyzed for alkaline phosphatase activity. In one experiment, ST-2 cells were allowed to recover for 24 h, treated with BMP-2 for 24 h, and analyzed for osteocalcin and runt-related transcription factor (Runx-2) mRNA expression. To test for effects on BMP or Wnt signaling, cells were allowed to recover for 24 h, transfected with BMP/Smad or Wnt/β-catenin reporter constructs, and treated with BMP or Wnt, as described under "Transient Transfections." Alternatively, cells were allowed to reach confluence, serum-deprived, and treated with BMP-2 for 20 min to test for effects on Smad1/5/8 phosphorylation by Western blot analysis.

Real-time Reverse Transcription-PCR—Total RNA was extracted from calvariae or cell cultures and mRNA levels determined by real-time RT-PCR (37, 38). For this purpose, 1–10 μg of RNA was reverse-transcribed using SuperScript III Platinum Two-Step qRT-PCR kit (Invitrogen), according to the manufacturer's instructions and amplified in the presence of 5′-CGGTTAGCCGCACTATCATCAAC[FAM]G-3′ and 5′-GTGAACTTCTTGGGCTTGCAGA-3′ primers for gremlin; 5′-CACTTACGGCGCTACCTTGGGTAAGT[FAM]G-3′ and 5′-CCCAGCACAACTCCTCCCTA-3′ primers for osteocalcin; 5′-CACAGGCGACAGTCCCAACTTCCTG[FAM]G-3′ and 5′-CACGGGCAGGGTCTTGTTG-3′ for Runx-2; 5′-CACTCCTGGTGAGCATCTTCGGAG[FAM]G-3′ and 5′-TCGTCGGTAAAGAAAGGCACAC-3′ for FGF-4; 5′-CACGCTCTGGAAAGCTGTGGCG[FAM]G-3′ and 5′-AGCTTCCCGTTCAGCTCTGG-3′ primers for glyceraldehyde-3-phosphate dehydrogenase (GAPDH) and Platinum Quantitative PCR SuperMix-UDG (Invitrogen) at 54–60 °C for 45 cycles. Gene copy number was estimated by comparison with a standard curve constructed using gremlin cDNA (Regeneron Pharmaceuticals) and corrected for *gapdh* (R. Wu, Ithaca, NY) copy number (17, 39). Reactions were conducted in a 96-well spectrofluorometric thermal iCycler (Bio-Rad), and fluorescence was monitored during every PCR cycle at the annealing step.

Alkaline Phosphatase Activity—Alkaline phosphatase activity (APA) was determined in cell extracts by the hydrolysis of *p*-nitrophenyl phosphate to *p*-nitrophenol, and measured by spectroscopy at 405 nm after 10 min of incubation at 25 °C, according to manufacturer's instructions (Sigma-Aldrich). Data are expressed as nanomoles of *p*-nitrophenol released per

minute per microgram of protein. Total protein content was determined in cell extracts by the DC protein assay in accordance with manufacturer's instructions (Bio-Rad).

Transient Transfections—To determine changes in BMP-2 signaling under conditions of gremlin RNAi, a construct containing 12 copies of a Smad 1/5 consensus sequence linked to an osteocalcin minimal promoter and a luciferase reporter gene (12×SBE-Oc-pGL3, M. Zhao, Antonio, TX) was tested in transient transfection experiments (40). To determine changes in Wnt/β-catenin transactivating activity, a construct containing 16 copies of the lymphoid enhancer binding factor/T-cell specific factor (Lef-1/Tcf-4) recognition sequence, cloned upstream of a minimal thymidine kinase promoter and a luciferase reporter gene (16×TCF-Luc, J. Billiard, Wyeth Research), was tested (41). ST-2 or MC3T3 cells were transiently transfected using FuGENE6 (3 μl of FuGENE:2 μg of DNA), according to manufacturer's instructions (Roche Applied Science) with 12×SBE-Oc-pGL3 or 16×TCF-Luc reporter construct (36). A cytomegalovirus (CMV)-directed β-galactosidase expression construct (Clontech, San Jose, CA) was used to control for transfection efficiency. Cells were exposed to the FuGENE-DNA mix for 16 h and transferred to serum-free medium for 6 h. Cells were then treated with BMP-2 or Wnt 3a for 24 h and harvested. Luciferase and β-galactosidase activities were measured using an Optocomp luminometer (MGM Instruments, Hamden, CT). Luciferase activity was corrected for β-galactosidase activity.

Western Blot Analysis—To determine the level of phosphorylation of Smad 1/5/8, the cell layer of ST-2 cells was washed with cold phosphate-buffered saline and extracted in cell lysis buffer (Cell Signaling Technology, Beverly, MA) in the presence of protease and phosphatase inhibitors, as described before (24). Protein concentrations were determined by DC protein assay, and 20 μg of total cellular protein was fractionated by gel electrophoresis in 10% polyacrylamide gels under reducing conditions, transferred to Immobilon P membranes (Millipore, Billerica, MA), which were blocked with 3% bovine serum albumin in phosphate-buffered saline. Membranes were exposed to a rabbit polyclonal antibody, which recognizes Smad 1, 5, and 8 phosphorylated at the last two serine residues (Cell Signaling Technology) or exposed to a monoclonal antibody to unphosphorylated Smad 1 (Santa Cruz Biotechnology, Santa Cruz, CA) at a 1:1000 dilution. Blots were then exposed to anti-rabbit or anti-mouse IgG antiserum conjugated to horseradish peroxidase (Sigma-Aldrich) and developed with a chemiluminescence detection reagent (PerkinElmer Life Sciences).

Statistical Analysis—Data are expressed as means ± S.E. Statistical significance was determined by Student's *t* test or analysis of variance.

RESULTS

Characterization of grem1-conditional Null Mice—Flanking with lox^P sites the segment of exon 2 encoding for gremlin was considered sufficient to generate a conditional null allele of *grem1*, because the entire coding sequence resides in this exon. Furthermore, this design was considered to be advantageous, because the deletion would mimic the *grem1* gene null alleles created previously, and the size of the deletion imparted by the Cre recombinase would be small, increasing the probability of excision (21, 22, 42). To monitor for the deletion of *grem1* in bone tissue, deletion of the lox^P-flanked region and suppressed levels of gremlin transcripts were documented in calvarial extracts from *grem1* conditional null mice ($grem1^{\Delta/LacZ}$). The mating scheme involved crossing homozygous osteocalcin Cre transgenics in a heterozygous null *grem1* background ($grem1^{+/LacZ}$:*Oc-Cre/Oc-Cre*) with homozygous $grem1^{loxP/loxP}$ mice. Consequently, deletion of the lox^P-flanked region was detected in calvarial extracts from the experimental cohort, $grem1^{\Delta/LacZ}$, and in extracts from littermate controls, $grem1^{\Delta/+}$ (Fig. 1*C*). No deletion of *grem1* sequences was detected in wild-type mice. Gremlin mRNA levels in calvarial extracts from 1-month-old $grem1^{\Delta/LacZ}$ conditional null mice were almost undetectable and markedly suppressed in relationship to those measured in littermate controls (Fig. 1*D*). LacZ staining of 3-day-old femurs and tibiae confirmed that gremlin is expressed during endochondral bone formation (Fig. 1*E*).

In accordance with their reported normal general phenotype, $grem1^{+/LacZ}$ haplo-insufficient mice did not exhibit a skeletal phenotype, as determined by bone histomorphometric analysis (Table 1) (22). Furthermore, $grem1^{loxP/loxP}$ homozygous mice were not different from wild-type controls, indicating that the 66-bp deletion engineered in the 3′-untranslated region, and the presence of lox^P sequences and selection cassette did not cause a skeletal phenotype. Consequently, $grem1^{\Delta/+}$ heterozygous littermate mice were considered appropriate controls for $grem1^{\Delta/LacZ}$ conditional null mice. 1-month-old $grem1^{\Delta/LacZ}$ conditional null mice appeared visually normal, had normal weight, and contact radiography did not reveal any obvious skeletal abnormalities (not shown). BMD was increased by 4–6% in $grem1^{\Delta/LacZ}$ conditional null mice, but it was not statistically different from the BMD obtained in $grem1^{\Delta/+}$ control littermates (Table 2).

Bone histomorphometric analysis of femurs from 1-month-old male $grem1^{\Delta/LacZ}$ conditional null mice revealed a 40% increase in trabecular bone volume, secondary to an increase in trabecular thickness and to a lesser extent in trabecular number (Table 3 and Fig. 2). The increase in bone volume observed was not associated with changes in osteoblast number. Osteoblast number/perimeter and osteoblast surface were not different from controls. Changes in trabecular bone volume were not associated with changes in bone resorption, because osteoclast number and eroded surface were normal. Fluorescence microscopy of $grem1^{\Delta/LacZ}$ conditional null male mice revealed increased mineral apposition and bone formation rates, indicating that the increased bone volume was secondary to an increase in osteoblast function. The skeletal phenotype of $grem1^{\Delta/LacZ}$ conditional null mice was transient and not observed in 3-month-old mice (data not shown). This was attributed to either a transient nature of the phenotype, which was evident in growing but not in mature mice, or to a possible decline in the activity of the osteocalcin promoter, used to direct the Cre recombinase, which is highest at 1 month of age (43, 44).

To investigate the impact of gremlin on osteoblastic cell differentiation and function, marrow stromal cells from $grem1^{\Delta/LacZ}$ conditional null and control mice were cultured

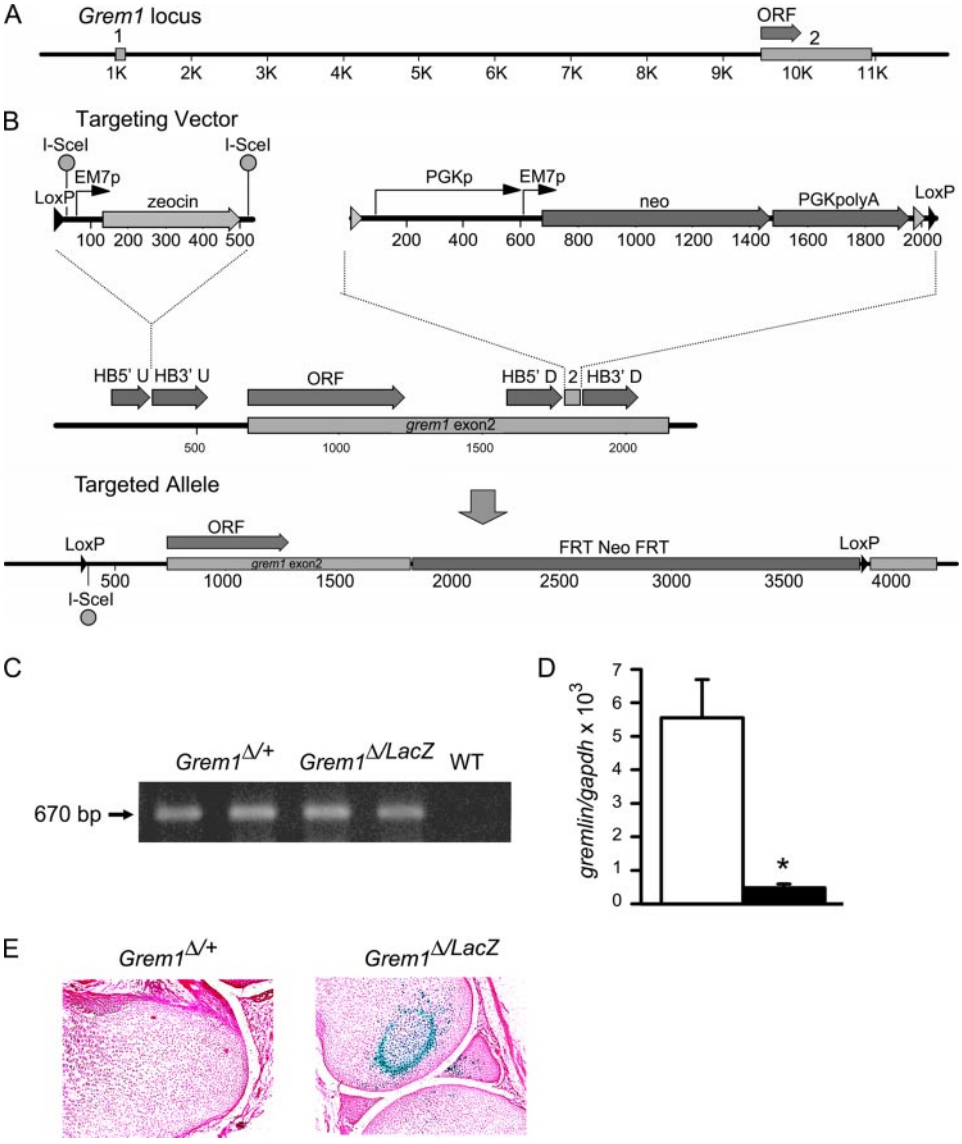

FIGURE 1. **Generation of the *grem1* conditional gene deletion.** *A* and *B*, schematic representation of the *grem1* locus and engineering of a *grem1* conditional null allele. In *A*, *boxes* show *grem1* exon 1 and 2 separated by an 8.5-kb intron. The *arrow* indicates the open reading frame (*ORF*) contained in exon 2. In *B*, the targeting vector engineered into a bacterial artificial chromosome (*BAC*), and the region surrounding exon 2 are shown. A lox^P site was inserted in a non-conserved region 335 bp upstream of exon 2, by introducing a LoxP I-SceI_EM7-Zeo_I-SceI cassette using homologous recombination; the cassette was removed by restricting with I-SceI, and re-ligation (not shown). The second lox^P site was inserted as part of a flippase recombinase target (*FRT*)-flanked phosphoglycerate kinase (*PGK*) neomycin phosphotransferase (Neo)-poly(A) lox^P cassette, containing polyadenylation and surrounding sequences of the mouse PKG gene, while deleting 66 bp of 3′-untranslated region to accommodate PCR probes for genotyping; this deletion does not disrupt or remove conserved elements. Transcription of Neo is directed by a PGK promoter for expression in mammalian cells or an $EM7_p$ promoter for expression in *Escherichia coli*. The 5′ and 3′ homologous boxes (*HB*) to introduce both cassettes are indicated. *C*, a representative PCR analysis of calvarial DNA from conditional *grem1* null ($grem1^{\Delta/LacZ}$) 1-month-old, heterozygous littermate ($grem1^{\Delta/+}$) control mice, and wild-type mice not bearing a $grem1^{loxP}$ allele. *D*, real-time RT-PCR of total RNA extracted from calvariae of 1-month-old conditional $grem1^{\Delta/LacZ}$ null (*black bars*) and heterozygous $grem1^{\Delta/+}$ littermate control (*white bars*) mice. RNA was amplified by real-time RT-PCR in the presence of specific primers to detect *grem1* and *gapdh*. Data are expressed as *grem1* copy number corrected for *gapdh* expression. *Bars* represent means ± S.E. for six observations. *, significantly different between $grem1^{\Delta/LacZ}$ conditional null mice and littermate $grem1^{\Delta/+}$ controls, $p < 0.05$. *E*, expression of gremlin in endochondral bone from 3-day-old mice. LacZ/β-galactosidase staining of whole mounts of femurs from $grem1^{\Delta/LacZ}$ conditional null and littermate $grem1^{\Delta/+}$ controls visualized by microscopy at final magnification of 100×.

for 10 and 16 days after confluence and treated, or not, with BMP-2 for the last 24 h of culture. Deletion of the lox^P flanked region was documented by PCR in DNA from cell extracts (not shown). Gremlin mRNA levels in cells from $grem1^{\Delta/LacZ}$ were markedly suppressed in relationship to control cells (Table 4). As the culture progressed, there was an increase in alkaline phosphatase activity in control cells. The conditional deletion of *grem1* caused an increase in alkaline phosphatase activity and enhanced the effect of BMP-2 (Table 4). The increase in basal activity probably represents sensitization to the effect of endogenous BMPs.

In Vitro Down-regulation of grem1 Expression—To determine mechanisms involved in the effect of gremlin on osteoblastic function, ST-2 stromal cells and MC3T3 osteoblastic cells were examined under conditions of gremlin down-regulation by RNAi. This resulted in suppression of gremlin transcripts by about 90% in ST-2 cells and by 60 to 90% in MC3T3 cells, when compared with basal levels of expression (Table 5, Fig. 3). To elucidate the mechanism of gremlin action, we analyzed the impact of gremlin down-regulation on downstream events of BMP-2 signaling and activity in ST-2 stromal and MC3T3 osteoblastic cells. In accordance with the skeletal phenotype observed, gremlin down-regulation enhanced the effect of BMP-2 on the transactivation of the Smad 1/5 dependent 12×SBE-Oc-pGL3 reporter construct in ST-2 cells. Consequently, the effect of BMP-2 on the transactivation of the 12×SBE-Oc-pGL3 reporter was 2.5 to 7 fold greater in the context of gremlin RNAi than under control conditions (Fig. 3*A*). In addition, gremlin down-regulation enhanced the stimulatory effect of BMP-2 on alkaline phosphatase activity and the effect of BMP-2 at 0.1 and 0.3 nM on the phosphorylation of Smad 1/5/8 in ST-2 cells (Fig. 3*C* and *E*). Down-regulation of gremlin also caused a modest increase in alkaline phosphatase activity in ST-2 cells under basal, non-BMP-2 treated, conditions. This probably represents sensitization to the effect of endogenous BMPs secreted by osteoblastic cells (45–47). BMP-2 at 3 nM overcame the sensitization caused by gremlin RNAi, possibly representing the effect of a maximally stimulatory dose of BMP-2 on Smad phosphorylation (48). In

TABLE 1

Femoral static and dynamic bone histomorphometry of *grem1* heterozygous (*grem1*$^{+/LacZ}$) mice and of *grem1*$^{loxP/loxP}$ and wild-type controls

Bone histomorphometry was performed on femurs from 1-month-old male *grem1*$^{+/LacZ}$ heterozygous or *grem1*$^{loxP/loxP}$ mice and wild-type littermate controls. For static histomorphometry, sections were stained with toluidine blue, and for dynamic histomorphometry unstained sections were analyzed by fluorescence microscopy. Values are means ± S.E.; $n = 5–8$.

	Wild type	*Grem1*$^{+/LacZ}$
Bone volume/total volume (%)	7.4 ± 0.7	7.1 ± 0.7
Trabecular number (/mm)	6.9 ± 0.5	7.1 ± 0.5
Trabecular thickness (/μm)	10.7 ± 0.6	9.8 ± 0.3
Osteoblasts/perimeter (/mm)	46 ± 3	50 ± 5
Osteoblast surface/bone surface (%)	23.8 ± 1.1	23.2 ± 1.9
Osteoclasts/perimeter (/mm)	9.9 ± 0.6	9.6 ± 0.6
Eroded surface/bone surface (%)	23.1 ± 1.0	22.0 ± 1.2
Mineral apposition rate (μm/day)	1.12 ± 0.11	1.13 ± 0.05
Bone formation rate/bone surface (μm^3/μm^2/day)	0.037 ± 0.011	0.029 ± 0.005
	Wild type	***Grem1*$^{loxP/loxP}$**
Bone volume/total volume (%)	7.4 ± 1.1	6.2 ± 0.6
Trabecular number (/mm)	7.2 ± 0.8	6.2 ± 0.6
Trabecular thickness (/μm)	10.0 ± 0.5	10.0 ± 0.2
Osteoblasts/perimeter (/mm)	52.9 ± 5.8	53.0 ± 6.3
Osteoblast surface/bone surface (%)	26.7 ± 2.7	26.5 ± 3.1
Osteoclasts/perimeter (/mm)	11.5 ± 1.4	11.5 ± 1.7
Eroded surface/bone surface (%)	24.6 ± 2.6	26.6 ± 1.4
Mineral apposition rate (μm/day)	1.04 ± 0.04	0.90 ± 0.06
Bone formation rate/bone surface (μm^3/μm^2/day)	0.035 ± 0.03	0.025 ± 0.03

TABLE 2

Weight and BMD (g/cm^2 × 10^4) in 1-month-old *grem1*$^{\Delta/LacZ}$ conditional null male mice and littermate (*grem1*$^{\Delta/+}$) controls

Values are means ± S.E.; $n = 9$.

	Weight	Total BMD	Vertebral BMD
	g	*g/cm^2 × 10^4*	
Grem1$^{\Delta/+}$	14.2 ± 0.7	352 ± 6	379 ± 11
Grem1$^{\Delta/LacZ}$	15.3 ± 0.8	367 ± 6	403 ± 15

TABLE 3

Femoral static and dynamic bone histomorphometry of *grem1*$^{\Delta/LacZ}$ conditional null male mice and *grem1*$^{\Delta/+}$ controls

Bone histomorphometry was performed on femurs from 1-month-old male *grem1*$^{\Delta/LacZ}$ conditional null mice and littermate *grem1*$^{\Delta/+}$ controls. For static histomorphometry, sections were stained with toluidine blue, and for dynamic histomorphometry unstained sections were analyzed by fluorescence microscopy. Values are means ± S.E.; $n = 5–9$.

	Grem1$^{\Delta/+}$	*Grem1*$^{\Delta/LacZ}$
Bone volume/total volume (%)	8.7 ± 0.8	12.1 ± 0.8[a]
Trabecular number (/mm)	8.3 ± 0.6	10.1 ± 0.7
Trabecular thickness (/μm)	10.5 ± 0.6	12.1 ± 0.4[a]
Osteoblasts/perimeter (/mm)	39 ± 2	38 ± 3
Osteoblast surface/bone surface (%)	19.0 ± 0.8	19.1 ± 1.0
Osteoclasts/perimeter (/mm)	10.7 ± 0.7	10.8 ± 0.7
Eroded surface/bone surface (%)	24.2 ± 1.4	24.0 ± 1.6
Mineral apposition rate (μm/day)	0.7 ± 0.08	0.9 ± 0.03[a]
Bone formation rate/bone surface (μm^3/μm^2/day)	0.010 ± 0.003	0.027 ± 0.005[a]

[a] Significantly different from controls, $p < 0.05$.

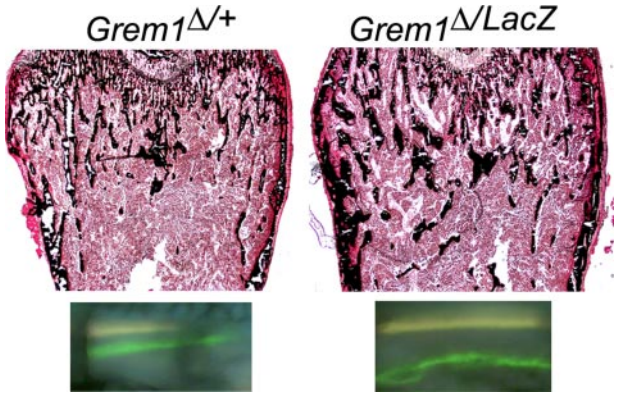

FIGURE 2. **Representative bone histomorphometry performed on femurs from 1-month-old male *grem1*$^{\Delta/LacZ}$ conditional null and littermate *grem1*$^{\Delta/+}$ controls stained with Von Kossa and visualization of calcein and demeclocycline labels by fluorescence microscopy at final magnifications of 40× and 400×, respectively.**

TABLE 4

Differentiation of bone marrow stromal cells from *grem1*$^{\Delta/LacZ}$ conditional null mice and *grem1*$^{\Delta/+}$ controls

Bone marrow stromal cells from 4-week-old *grem1*$^{\Delta/+}$ and *grem1*$^{\Delta/LacZ}$ were cultured to confluence, switched to differentiation medium, and cultured for an additional 10- or 16-day period. Cultures were serum-deprived overnight and treated or not with BMP-2 for 24 h. Deletion of *lox*^{P}-flanked sequences was documented by PCR analysis of DNA from cell extracts. The *grem1* copy number was determined by real-time RT-PCR and corrected for *gapdh* expression. APA was quantified in cell extracts and is expressed as nanomoles of *p*-nitrophenol/min/μg of total protein. Values are means ± S.E. for 3 (*grem1* copy number) or 6 (APA) observations.

	10 days post confluence		16 days post confluence	
	Grem1$^{\Delta/+}$	*Grem1*$^{\Delta/LacZ}$	*Grem1*$^{\Delta/+}$	*Grem1*$^{\Delta/LacZ}$
	nmol/min/μg protein			
APA				
Control	197 ± 25	395 ± 33[a]	290 ± 31	666 ± 32[a]
BMP-2, 0.3 nM	231 ± 40	370 ± 60	396 ± 77	946 ± 56[a]
BMP-2, 3 nM	274 ± 40	404 ± 33[a]	361 ± 50	725 ± 72[a]
grem1/gapdh				
Control	2.2 ± 0.9	<0.1	0.7 ± 0.07	0.1 ± 0.05[a]

[a] Significantly different from controls, $p < 0.05$.

TABLE 5

Effect of gremlin down-regulation by RNA interference on gremlin mRNA expression in ST-2 and MC3T3 cells

ST-2 or MC3T3 cells were cultured to subconfluence and transfected with gremlin or control scrambled small interfering RNAs (siRNA). The *grem1* copy number was determined by real-time RT-PCR, corrected for *gapdh* copy number and expressed as % of scrambled control. Values are means ± S.E.; $n = 3–5$, except for MC3T3 cells, where scrambled at 72 h and gremlin at 96 h was $n = 2$. Data for ST-2 cells were pooled from two experiments.

Hours after siRNA	*grem1/gapdh*			
	ST-2 cells		MC3T3 cells	
	Scrambled	Gremlin	Scrambled	Gremlin
24	100 ± 5.7	6.63 ± 1.9	100 ± 14.6	3.5 ± 0.9
48	100 ± 13.2	8.42 ± 1.9	100 ± 4.1	4.0 ± 0.2
72	100 ± 12.8	5.43 ± 1.6	100 ± 7.4	6.4 ± 2.9
96	100 ± 6.9	4.52 ± 1.9	100 ± 8.7	7.1 ± 0.6

accordance with the results obtained in ST-2 cells, gremlin down-regulation in MC3T3 cells enhanced the stimulatory effect of BMP-2 on the transactivation of the 12×SBE-Oc-pGL3 reporter by 2 to 7 fold and on alkaline phosphatase activity by about 1.5 fold (Fig. 3*B* and *D*). These results indicate that gremlin is an endogenous BMP antagonist that opposes BMP effects on Smad signaling and on osteoblast maturation and function. In accordance with these effects, down-regulation of gremlin in ST-2 cells enhanced the stimulatory effect of BMP-2 on osteocalcin and Runx-2 mRNA expression (Table 6).

To explore additional mechanisms involved in the effects of gremlin on cells of the osteoblastic lineage, we tested whether its down-regulation modified Wnt/β-catenin signaling and Wnt effects in ST-2 stromal cells, which are less differentiated and more responsive to Wnt 3 than the more mature MC3T3 cells (32, 33, 36). Wnt 3a caused a dose dependent increase in

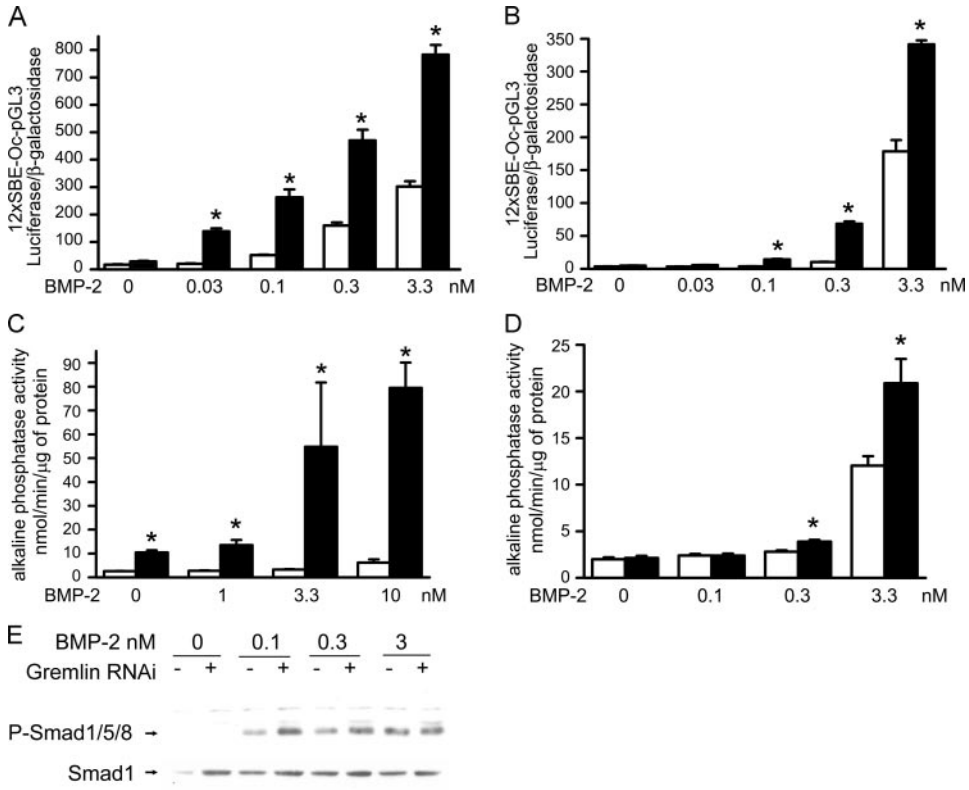

FIGURE 3. **Effect of gremlin down-regulation by RNA interference on BMP-2 signaling and activity in ST-2 stromal and MC3T3 cells.** ST-2 (*A*, *C*, and *E*) or MC3T3 (*B* and *D*) cells were cultured to subconfluence and transfected with gremlin or control scrambled small interfering RNAs (siRNA). Down-regulation of gremlin mRNA was documented in parallel cultures by real-time RT-PCR at the completion of the experiment. Gremlin mRNA levels determined in duplicate parallel samples were suppressed from 1.8 to 0.2 (*A*), 0.4 to 0.03 (*C*), 3.7 to 0.3 (*E*), 1.4 to 0.6 (*B*), and 2.0 to 0.1 (*D*) *grem1/gapdh* copies in cells transfected with control scrambled or gremlin siRNA, respectively. *A* and *B*, cells were transfected with 12×SBE-Oc-pGL3 and a CMV/β-galactosidase expression vector, 24 h after transfecting the siRNAs. Cells were switched to α-MEM for 6 h and exposed to control medium or BMP-2 at the indicated doses for 24 h. Data shown represent luciferase/β-galactosidase activity for cells transfected with scrambled siRNA (*white bars*) or gremlin siRNA (*black bars*). *Bars* represent means ± S.E. for six observations. *C* and *D*, cells were exposed to control medium or BMP-2 at the indicated doses, 24 h after transfecting the siRNAs, cultured for 72 h and APA quantified in extracts from cells transfected with scrambled siRNA (*white bars*) or gremlin siRNA (*black bars*). APA is expressed as nanomoles of *p*-nitrophenol/min/μg of total protein. *Bars* represent means ± S.E. for six observations. *E*, cells were exposed to control medium or BMP-2 at the indicated doses for 20 min 72 h after transfecting the siRNAs, and cell lysates were examined for the presence of phosphorylated Smad 1/5/8 or unphosphorylated Smad 1 by Western blot analysis. *, significantly different between cells transfected with scrambled and gremlin siRNA ($p < 0.05$).

TABLE 6

Effect of gremlin down-regulation by RNAi on osteocalcin and Runx-2 expression in ST-2 stromal cells

ST-2 cells were cultured to subconfluence and transfected with gremlin or control scrambled small interfering RNAs (siRNA). Cells were exposed to control medium or to BMP-2 at 0.3 nM, 24 h after transfecting the siRNAs, cultured for 24 h, and RNA was extracted and quantified. Data are expressed as *osteocalcin*, *runx-2*, and *grem1* copy number, determined by real-time RT-PCR, corrected for *gapdh* expression. Values are means ± S.E.; $n = 3$.

	Scrambled RNAi	Gremlin RNAi
osteocalcin/gapdh		
Control	1.1 ± 0.4	2.1 ± 0.4
BMP-2	0.8 ± 0.5	4.1 ± 0.3[a]
runx-2/gapdh		
Control	1.1 ± 0.6	3.0 ± 0.2[a]
BMP-2	0.9 ± 0.3	4.3 ± 1.2[a]
grem1/gapdh		
Control	8.9 ± 3.1	0.8 ± 0.1 ($p < 0.057$)
BMP-2	9.0 ± 2.4	0.9 ± 0.1[a]

[a] Significantly different from controls, $p < 0.05$.

the transactivation of the Wnt/β-catenin dependent 16×TCF-Luc reporter construct and on alkaline phosphatase activity (Fig. 4*A* and *B*). Gremlin down-regulation enhanced the stimulatory effect of Wnt 3a on the transactivation of the Wnt dependent 16×TCF-Luc reporter construct by 2.5 to 3.5 fold and on alkaline phosphatase activity by 1.5 to 2 fold, indicating that gremlin has BMP and Wnt/β-catenin antagonizing activity.

Gremlin down-regulation did not modify the expression of FGF-4 in ST-2 cells, and FGF-4 transcripts were virtually undetectable in MC3T3 cells. In an experiment where gremlin mRNA levels were suppressed by >90% following gremlin RNAi, the expression of FGF-4 was (means ± S.E.; $n = 3$) 0.75 ± 0.2 *fgf-4/gapdh* copies in control ST-2 cells and 0.85 ± 0.1 *fgf-4/gapdh* copies in gremlin-silenced ST-2 cells. Levels of SHH mRNA in ST-2 cells were undetectable (data not shown).

DISCUSSION

Our findings demonstrate that the conditional deletion of the BMP antagonist gremlin, in the skeletal environment, causes increased trabecular bone volume secondary to increased bone formation and osteoblastic activity. This is the converse phenotype of that displayed by transgenic mice overexpressing gremlin under the control of the osteoblastic specific osteocalcin promoter, which caused an inhibition of bone formation and marked osteopenia (24). *Grem1* haplo-insufficiency did not cause a skeletal phenotype, and this is in accordance with the lack of observable limb developmental abnormalities or other apparent phenotypic alterations in *grem1* heterozygous mice (21, 22). Although studies in *grem1* null mice have demonstrated a role of gremlin in cell survival during limb and kidney organogenesis, conditional deletion of the *grem1* gene in the post natal bone environment did not result in a change in osteoblast number (22). The skeletal phenotype of *grem1* conditional null male mice was transient and observed at 1 month, but not at 3 months of age. This could be attributed to the decline in the activity of the osteocalcin promoter directing the Cre recombinase (43, 44). However, it is possible that gremlin plays a more significant role during the early phases of skeletal growth, and a lesser effect in the adult skeleton. It is of interest that the conditional deletion of *grem1* did not cause an obvious skeletal phenotype in 1-month-old female mice (data not shown). Recently, we reported marked age-related differences in the trabecular bone structure of C57BL/6J mice and noted a particularly unstable phenotype in wild-type young female mice with

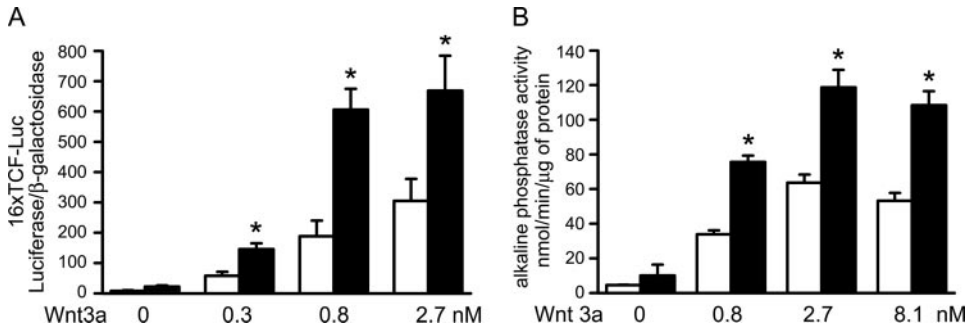

FIGURE 4. **Effect of gremlin down-regulation by RNA interference on Wnt 3a signaling and activity in ST-2 stromal cells.** ST-2 cells were cultured to subconfluence and transfected with gremlin or control scrambled small interfering RNA (siRNA). Down-regulation of gremlin mRNA was documented in parallel cultures by real-time RT-PCR at the completion of the experiment. Gremlin mRNA levels determined in duplicate parallel samples were suppressed from 4.3 to 1.2 (*A*) and 4.7 to 0.1 (*B*) *grem1/gapdh* copies in cells transfected with control scrambled or gremlin siRNA, respectively. *A*, cells were transfected with 16×TCF-Luc and CMV/β-galactosidase expression vector, 24 h after transfecting the siRNAs. Cells were switched to α-MEM for 6 h and exposed to control medium or Wnt 3a at 0.3 to 2.7 nM for 24 h. Data shown represent luciferase/β-galactosidase activity for cells transfected with scrambled siRNA (*white bars*) or gremlin siRNA (*black bars*). *B*, cells were exposed to control medium or Wnt 3a at 0.8 to 8.1 nM, 24 h after transfecting the siRNAs and cultured for 72 h, and APA was quantified in extracts from cells transfected with scrambled RNA (*white bars*) or gremlin siRNA (*black bars*). APA is expressed as nanomoles of *p*-nitrophenol/min/μg of total protein. *Bars* represent means ± S.E.; $n = 6$ observations. *, significantly different between cells transfected with scrambled and gremlin siRNA ($p < 0.05$).

an early loss of trabecular bone occurring at 1 to 2 months of age (49). This was not observed in male mice, which displayed a more stable trabecular bone architecture in the first few months of life. The rapid loss of trabecular bone might have precluded the detection of a phenotype in female mice despite *grem1* deletion as documented by PCR of calvarial DNA and suppressed gremlin transcripts in calvarial extracts (not shown). It appears that the deletion of *grem1* could not overcome the loss of bone occurring after peak trabecular bone mass was reached. Our observations would suggest that the *grem1* deletion has a major impact in the early phases of bone acquisition, and are in accordance with the role of BMPs during skeletal development (50).

The *in vivo* skeletal phenotype of $grem1^{\Delta/LacZ}$ conditional null male mice is consistent with previous studies indicating that gremlin is a BMP antagonist in the skeleton. The *in vivo* findings were confirmed by parallel *in vitro* experiments in marrow stromal cells from $grem1^{\Delta/LacZ}$ and in osteoblastic cell lines, where gremlin expression was down-regulated using RNAi. In previous work, we demonstrated that the addition of gremlin to stromal and osteoblastic cell lines inhibits BMP and Wnt signaling and activity, and that marrow stromal cells from transgenics overexpressing gremlin display a decrease in osteoblastic cell differentiation and function (24). Conversely, marrow stromal cells from $grem1^{\Delta/LacZ}$ exhibited increased alkaline phosphatase activity, a marker of osteoblastic differentiation, and increased responsiveness to BMP-2. Accordingly, down-regulation of gremlin in cells of the osteoblastic lineage caused an increased response to BMP on Smad signaling, alkaline phosphatase activity, and osteoblast gene markers, confirming that gremlin is an inhibitor of BMP activity and osteoblastic function. In osteoblasts, Wnt signals through the canonical Wnt/β-catenin pathway stabilizing β-catenin, which in turn translocates to the nucleus, where it associates with members of the TCF/LEF family to activate expression of Wnt-responsive genes (4, 9, 10). The addition of gremlin to cell cultures inhibits the transactivation of Wnt/β-catenin reporter constructs (24). Conversely, down-regulation of gremlin results in increased Wnt/β-catenin signaling and activity. This sensitization of Wnt/β-catenin signaling could imply direct interactions of gremlin with Wnt or Wnt receptors/co-receptors. Members of the dan/cerberus family of BMP antagonists can inhibit BMP as well as Wnt signaling and activity (13–16). However, direct interactions between gremlin and Wnt and its receptors have not been reported, and therefore the possibility remains that the effect of Gremlin on Wnt signaling is mediated through its suppression of BMP signaling or through as yet undiscovered mechanisms. The sensitization of Wnt signaling by the removal of a BMP antagonist is not surprising, in view of the close relationship between BMP-2 and Wnt effects in cells of the osteoblastic lineage, but the exact mechanisms involved are not fully elucidated, because BMP and Wnt signal through independent pathways.

Although overexpression of various BMP/Wnt antagonists in the skeletal environment can lead to osteopenia, their ultimate physiological role in bone is probably distinct and dependent on their mechanism of action and patterns and levels of expression by skeletal cells (24, 51–53). Gremlin is important in the regulation of BMP activity and skeletal physiology and may have additional functions. Gremlin is expressed by selected cancer-associated stromal cells and has been postulated to favor tumor cell survival and expansion (20). The results observed in mice and cells misexpressing gremlin can be explained by its capacity to bind and block the actions of BMP-2, -4, and -7; however, BMP-independent biological effects of gremlin have not been completely excluded (1, 17). Recent work in endothelial cells has demonstrated pro-angiogenic activity of gremlin and has provided evidence for direct binding of gremlin to endothelial cells and the activation of extracellular regulated kinases (ERK) 1/2 (54). ERK1/2 phosphorylates non-activating sites of Smad, reducing the nuclear accumulation of Smads and their effects on transcription and could contribute to the BMP antagonistic activity of gremlin (55, 56).

In conclusion, gremlin is a physiological antagonist of BMPs in the skeleton, and its deletion or down-regulation sensitizes skeletal cells to the actions of BMP and Wnt, and enhances bone formation *in vivo*.

Acknowledgments—We thank T. Clemens for transgenics expressing Cre recombinase, R. Harland for gremlin heterozygous null mice, Wyeth Research for BMP-2 and 16×TCF-Luc construct, M. Zhao for 12×SBE-Oc-pGL3 reporter construct, I. Kalajzic for helpful advice, M. Burton and E. Paul for technical help, and M. Yurczak for secretarial assistance.

REFERENCES

1. Canalis, E., Economides, A. N., and Gazzerro, E. (2003) *Endocr. Rev.* **24,** 218–235
2. Thies, R. S., Bauduy, M., Ashton, B. A., Kurtzberg, L., Wozney, J. M., and Rosen, V. (1992) *Endocrinology* **130,** 1318–1324
3. Ghosh-Choudhury, N., Harris, M. A., Feng, J. Q., Mundy, G. R., and Harris, S. E. (1994) *Crit. Rev. Eukaryot. Gene Expr.* **4,** 345–355
4. Westendorf, J. J., Kahler, R. A., and Schroeder, T. M. (2004) *Gene* (*Amst.*) **341,** 19–39
5. Miyazono, K. (1999) *Bone* **25,** 91–93
6. Nohe, A., Keating, E., Knaus, P., and Petersen, N. O. (2004) *Cell Signal* **16,** 291–299
7. Nohe, A., Hassel, S., Ehrlich, M., Neubauer, F., Sebald, W., Henis, Y. I., and Knaus, P. (2002) *J. Biol. Chem.* **277,** 5330–5338
8. Lai, C. F., and Cheng, S. L. (2002) *J. Biol. Chem.* **277,** 15514–15522
9. Krishnan, V., Bryant, H. U., and MacDougald, O. A. (2006) *J. Clin. Invest.* **116,** 1202–1209
10. Wodarz, A., and Nusse, R. (1998) *Annu. Rev. Cell Dev. Biol.* **14,** 59–88
11. Gazzerro, E., and Canalis, E. (2006) *Rev. Endocr. Metab. Disord.* **7,** 51–65
12. Kawano, Y., and Kypta, R. (2003) *J. Cell Sci.* **116,** 2627–2634
13. Winkler, D. G., Sutherland, M. S., Ojala, E., Turcott, E., Geoghegan, J. C., Shpektor, D., Skonier, J. E., Yu, C., and Latham, J. A. (2005) *J. Biol. Chem.* **280,** 2498–2502
14. Li, X., Zhang, Y., Kang, H., Liu, W., Liu, P., Zhang, J., Harris, S. E., and Wu, D. (2005) *J. Biol. Chem.* **280,** 19883–19887
15. Laurikkala, J., Kassai, Y., Pakkasjarvi, L., Thesleff, I., and Itoh, N. (2003) *Dev. Biol.* **264,** 91–105
16. Bell, E., Munoz-Sanjuan, I., Altmann, C. R., Vonica, A., and Brivanlou, A. H. (2003) *Development* **130,** 1381–1389
17. Hsu, D. R., Economides, A. N., Wang, X., Eimon, P. M., and Harland, R. M. (1998) *Mol. Cell* **1,** 673–683
18. Topol, L. Z., Bardot, B., Zhang, Q., Resau, J., Huillard, E., Marx, M., Calothy, G., and Blair, D. G. (2000) *J. Biol. Chem.* **275,** 8785–8793
19. Topol, L. Z., Marx, M., Laugier, D., Bogdanova, N. N., Boubnov, N. V., Clausen, P. A., Calothy, G., and Blair, D. G. (1997) *Mol. Cell Biol.* **17,** 4801–4810
20. Sneddon, J. B., Zhen, H. H., Montgomery, K., van de, R. M., Tward, A. D., West, R., Gladstone, H., Chang, H. Y., Morganroth, G. S., Oro, A. E., and Brown, P. O. (2006) *Proc. Natl. Acad. Sci. U. S. A.* **103,** 14842–14847
21. Khokha, M. K., Hsu, D., Brunet, L. J., Dionne, M. S., and Harland, R. M. (2003) *Nat. Genet.* **34,** 303–307
22. Michos, O., Panman, L., Vintersten, K., Beier, K., Zeller, R., and Zuniga, A. (2004) *Development* **131,** 3401–3410
23. Pereira, R. C., Economides, A. N., and Canalis, E. (2000) *Endocrinology* **141,** 4558–4563
24. Gazzerro, E., Pereira, R. C., Jorgetti, V., Olson, S., Economides, A. N., and Canalis, E. (2005) *Endocrinology* **146,** 655–665
25. Valenzuela, D. M., Murphy, A. J., Frendewey, D., Gale, N. W., Economides, A. N., Auerbach, W., Poueymirou, W. T., Adams, N. C., Rojas, J., Yasenchak, J., Chernomorsky, R., Boucher, M., Elsasser, A. L., Esau, L., Zheng, J., Griffiths, J. A., Wang, X., Su, H., Xue, Y., Dominguez, M. G., Noguera, I., Torres, R., Macdonald, L. E., Stewart, A. F., DeChiara, T. M., and Yancopoulos, G. D. (2003) *Nat. Biotechnol.* **21,** 652–659
26. Zhang, Y., Buchholz, F., Muyrers, J. P., and Stewart, A. F. (1998) *Nat. Genet.* **20,** 123–128
27. Zhang, M., Xuan, S., Bouxsein, M. L., von Stechow, D., Akeno, N., Faugere, M. C., Malluche, H., Zhao, G., Rosen, C. J., Efstratiadis, A., and Clemens, T. L. (2002) *J. Biol. Chem.* **277,** 44005–44012
28. Soriano, P. (1999) *Nat. Genet.* **21,** 70–71
29. Nagy, T. R., Prince, C. W., and Li, J. (2001) *J. Bone Miner. Res.* **16,** 1682–1687
30. Parfitt, A. M., Drezner, M. K., Glorieux, F. H., Kanis, J. A., Malluche, H., Meunier, P. J., Ott, S. M., and Recker, R. R. (1987) *J. Bone Miner. Res.* **2,** 595–610
31. Adams, N. C., and Gale, N. W. (2006) in *Principle and Practice Mammalian and Avian Trangenesis–New Approaches* (Pease, S., and Lois, C., eds) pp. 131–172, Springer-Verlag, New York
32. Otsuka, E., Yamaguchi, A., Hirose, S., and Hagiwara, H. (1999) *Am. J. Physiol.* **277,** C132–C138
33. Sudo, H., Kodama, H. A., Amagai, Y., Yamamoto, S., and Kasai, S. (1983) *J. Cell Biol.* **96,** 191–198
34. Sharp, P. A. (2001) *Genes Dev.* **15,** 485–490
35. Elbashir, S. M., Harborth, J., Lendeckel, W., Yalcin, A., Weber, K., and Tuschl, T. (2001) *Nature* **411,** 494–498
36. Deregowski, V., Gazzerro, E., Priest, L., Rydziel, S., and Canalis, E. (2006) *J. Biol. Chem.* **281,** 6203–6210
37. Nazarenko, I., Pires, R., Lowe, B., Obaidy, M., and Rashtchian, A. (2002) *Nucleic Acids Res.* **30,** 2089–2195
38. Nazarenko, I., Lowe, B., Darfler, M., Ikonomi, P., Schuster, D., and Rashtchian, A. (2002) *Nucleic Acids Res.* **30,** e37
39. Tso, J. Y., Sun, X. H., Kao, T. H., Reece, K. S., and Wu, R. (1985) *Nucleic Acids Res.* **13,** 2485–2502
40. Zhao, M., Qiao, M., Harris, S. E., Oyajobi, B. O., Mundy, G. R., and Chen, D. (2004) *J. Biol. Chem.* **279,** 12854–12859
41. Billiard, J., Way, D. S., Seestaller-Wehr, L. M., Moran, R. A., Mangine, A., and Bodine, P. V. (2005) *Mol. Endocrinol.* **19,** 90–101
42. Ringrose, L., Chabanis, S., Angrand, P. O., Woodroofe, C., and Stewart, A. F. (1999) *EMBO J.* **18,** 6630–6641
43. Frenkel, B., Capparelli, C., Van Auken, M., Baran, D., Bryan, J., Stein, J. L., Stein, G. S., and Lian, J. B. (1997) *Endocrinology* **138,** 2109–2116
44. Devlin, R. D., Du, Z., Buccilli, V., Jorgetti, V., and Canalis, E. (2002) *Endocrinology* **143,** 3955–3962
45. Harris, S. E., Sabatini, M., Harris, M. A., Feng, J. Q., Wozney, J., and Mundy, G. R. (1994) *J. Bone Miner. Res.* **9,** 389–394
46. Pereira, R. C., Rydziel, S., and Canalis, E. (2000) *J. Cell Physiol.* **182,** 239–246
47. Gazzerro, E., Rydziel, S., and Canalis, E. (1999) *Endocrinology* **140,** 562–567
48. Gazzerro, E., Deregowski, V., Vaira, S., and Canalis, E. (2005) *Endocrinology* **146,** 3875–3882
49. Glatt, V., Canalis, E., Stadmeyer, L., and Bouxsein, M. L. (2007) *J. Bone Miner. Res.* **22,** 1197–1207
50. Bandyopadhyay, A., Tsuji, K., Cox, K., Harfe, B. D., Rosen, V., and Tabin, C. J. (2006) *PLoS. Genet.* **2,** e216
51. Devlin, R. D., Du, Z., Pereira, R. C., Kimble, R. B., Economides, A. N., Jorgetti, V., and Canalis, E. (2003) *Endocrinology* **144,** 1972–1978
52. Li, J., Sarosi, I., Cattley, R. C., Pretorius, J., Asuncion, F., Grisanti, M., Morony, S., Adamu, S., Geng, Z., Qiu, W., Kostenuik, P., Lacey, D. L., Simonet, W. S., Bolon, B., Qian, X., Shalhoub, V., Ominsky, M. S., Zhu, K. H., Li, X., and Richards, W. G. (2006) *Bone* **39,** 754–766
53. Baron, R., Rawadi, G., and Roman-Roman, S. (2006) *Curr. Top Dev. Biol.* **76,** 103–127
54. Stabile, H., Mitola, S., Moroni, E., Belleri, M., Nicoli, S., Coltrini, D., Peri, F., Pessi, A., Orsatti, L., Talamo, F., Castronovo, V., Waltregny, D., Cotelli, F., Ribatti, D., and Presta, M. (2007) *Blood* **109,** 1834–1840
55. Kretzschmar, M., Doody, J., and Massague, J. (1997) *Nature* **389,** 618–622
56. Osyczka, A. M., and Leboy, P. S. (2005) *Endocrinology* **146,** 3428–3437